Wide Optical Beam Steering LCOS Device for Solid-State LiDAR Applications

Seong-Jin Son, Toijam Sunder Meetei, Byeongchan Park, Yong-Tak Lee, Nan Ei Yu, and Do-Kyeong Ko

***Abstract*— We demonstrate one-dimensional beam steering in a liquid crystal on silicon (LCOS) device with a large birefringence (Δn = 0.2028 at 1550 nm) of the liquid crystal (LC) mixture. The experimental analysis of the optical beam steering angles at different LCOS grating periods is reported. A maximum beam steering angle of ±15.6° is measured for the fine grating pitch of 3.6 μm with a 1^{st}-order diffraction efficiency (η_1) of 2.28%. Also, the experimental results obtained were verified with the grating equation and numerical simulation. The wide optical beam steering capabilities of our fabricated LCOS device show great potential applications in solid-state LiDAR for future autonomous vehicles.**

***Index Terms*— Liquid crystal on silicon, solid-state LiDAR, optical beam steering, diffraction efficiency.**

I. Introduction

RECENTLY, the automotive industry has been shifting its attention to making smarter cars. Not only major automotive vendors but also electronic and IT companies such as Google, IBM, Intel, and Samsung are pushing their boundaries to enter the new era of the emerging automotive industry market. Many advanced driver assistance systems (ADAS) have already been used in the automotive industry for the safety and convenience of the driving experience [1]. ADAS technology is popular at the initial stage of autonomous driving, usually named Level 2 [2]. In the next few years, Level 3 autonomous driving markets are expected to open. In Level 3, the car must drive autonomously, but the driver can take control over all driving functions under certain circumstances. The essential technology of Level 3 is the light detection and ranging (LiDAR) sensor, which generates 3D spatial information to detect distances and movements of surrounding pedestrians and cars by observing the time interval taken between the emission and receiving of laser light [2]. Although other sensors, such as a camera sensor or radio detection and ranging (RADAR), can be used for Level 3, but not suitable for reliable operations. This is because the camera sensors can confuse distinguishing between bright colors from incoming trailers and the sunny sky as well as highly dependent on the environmental conditions [3]. In addition, RADAR sensors have disadvantages in precisely locating the objects due to their longer operating wavelength [4]. On the other hand, the commercially available mechanical LiDAR system is not so attractive in the current market due to its bulky size, limited imaging rates, and expensive. To counter this issue, solid-state LiDAR has drawn much attention due to its miniaturized footprint, low cost, and lack of mechanically rotating parts to scan or steer the laser beams [5]. Besides, solid-state LiDAR devices have huge potential from a market perspective with mass production using a semiconductor foundry.

Lately, all-solid-state LiDAR systems realized by optical phased array (OPA) has been an interesting approach for beam steering applications. Various optical beam steering methods via OPA technology have been developed, such as microelectromechanical system (MEMS) OPA, metasurface (meta) OPA, photonic integrated chip (PIC) OPA, and liquid crystal (LC) OPA [6]. MEMS-OPA had a great impact in reducing the cost, energy consumption, and high scanning speed of the solid-state LiDAR system, but fundamentally closer to mechanical steering and is therefore vulnerable to vibration [7]. The meta-OPA, where the amplitude, phase, and polarization states of the light can be manipulated with extreme freedom on an ultra-thin and flat form factor metasurface [8], [9]. The PIC-OPA utilizes the thermo-optic or electro-optic effect to control the optical phase and steer the constructively interfered coherent light emitted from each antenna in the target direction [10], [11].

The LC-OPA device is more attractive due to its low cost, high resolution, lightweight, low profile, low power consumption, and industrially mature manufacturing availability. In addition, LC-OPA provides an appropriate FOV and steering speed at the kHz level. C. Sun et al. have demonstrated a liquid crystal on insulator (LCOS) device with a high diffraction efficiency of 56.6% at a deflection angle of 4.5° for a 1550 nm wavelength [12]. Further, the total optical efficiency of the phase-only LCOS device was improved by a multi-layer dielectric mirror coating to maximize its reflectance from ∼80% to >96%, which is 12%-18% higher than the standard

Manuscript received 21 September 2023; accepted 2 November 2023. Date of publication 8 November 2023; date of current version 4 December 2023. This work was supported in part by the National IT Industry Promotion Agency of Korea (NIPA) funded by the Ministry of Science and ICT (MSIT) under Grant S0315-21-1001-C01; in part by the National Research Foundation of Korea (NRF) Grant funded by the Korean Government, MSIT, under Grant 2021R1A2C100713011; in part by the Korea Evaluation Institute of Industrial Technology (KEIT) Grant funded by the Korea Government (MOTIE) under Grant 1415181752; and in part by the GIST Research Institute (GRI) under Grant 2023. *(Corresponding authors: Nan Ei Yu; Do-Kyeong Ko.)*

Seong-Jin Son is with the Department of Physics and Photon Science, Gwangju Institute of Science and Technology, Gwangju 61005, South Korea.

Toijam Sunder Meetei, Byeongchan Park, Yong-Tak Lee, and Nan Ei Yu are with the Advanced Photonics Research Institute, Gwangju Institute of Science and Technology, Gwangju 61005, South Korea (e-mail: neyu@gist.ac.kr).

Do-Kyeong Ko is with the Department of Physics and Photon Science and the Advanced Photonics Research Institute, Gwangju Institute of Science and Technology, Gwangju 61005, South Korea (e-mail: dkko@gist.ac.kr).

Color versions of one or more figures in this letter are available at https://doi.org/10.1109/LPT.2023.3330800.

Digital Object Identifier 10.1109/LPT.2023.3330800

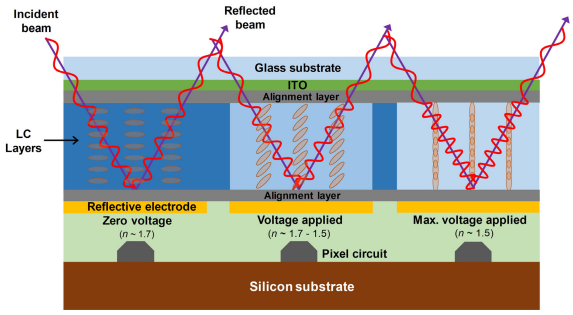

Fig. 1. Schematic representation of the LCOS device for optical beam steering.

LCOS device [13]. Also, researchers have reported various approaches to increasing the diffraction efficiency and steering angle of the LCOS device [14], [15], [16], [17]. However, a wider beam steering angle with an easy fabrication process is needed for a solid-state LiDAR system. In this letter, we demonstrate a wide-angle non-mechanical beam steering device using LCOS for solid-state LiDAR applications. The fine LCOS pixel size of the proposed device provides a wide FOV of about 31.2°. A beam steering angle (θ) of about ~15.6° was achieved at the 1550 nm wavelength for the lowest pixel of the LCOS device.

II. Operation Principle and Device Design

The optical beam steering using an LCOS device exploits the birefringence of LC material to modulate the phase of the incident light [18]. Since the birefringent property of the LCOS can be controlled electrically, the LC exhibits an ordinary (n_o) and extraordinary (n_e) refractive index of 1.4954 and 1.6982 at 1550 nm wavelength, respectively, with an index difference ($\Delta n = n_o - n_e$) of 0.2028. This leads to a change in the optical path of the incident beam due to a variation in the refractive index. Furthermore, a constant voltage is applied to each pixel to control the phase delay of the individual pixel in the LCOS device. The electric field aligns the LC direction perpendicular to the glass substrate [19], which results in a change in the effective external refractive index of the LC for different orientations of the LC direction. Therefore, a periodic diffraction grating structure is constructed by applying a periodic voltage to the LCOS device. For a periodic diffraction grating, the angle of the first-order diffraction pattern can be calculated using the grating equation as [20],

$$d(\sin\alpha + \sin\beta) = m\lambda \tag{1}$$

where, d is period of grating, α is incidence angle, β is diffraction angle, m is diffraction order ($m = 1$, only first-order is considered in our entire work), and λ is the operating wavelength.

The LCOS device has been fabricated by MAY Co., Ltd. It consists of a layer of LC material between the top cover glass (soda lime) and the silicon backplane, as shown in Fig. 1. For voltage applications, the LCOS has a 200 Å layer of ITO under the 0.7 mm thick cover glass coated with anti-reflection at 1550 nm wavelength. The pixel gap and cell gap are 0.432 μm and 5.6 μm, respectively. The phase depth of the blazed grating on the LCOS operation is 1.4π. On the silicon backplane, the transistors are hidden behind a

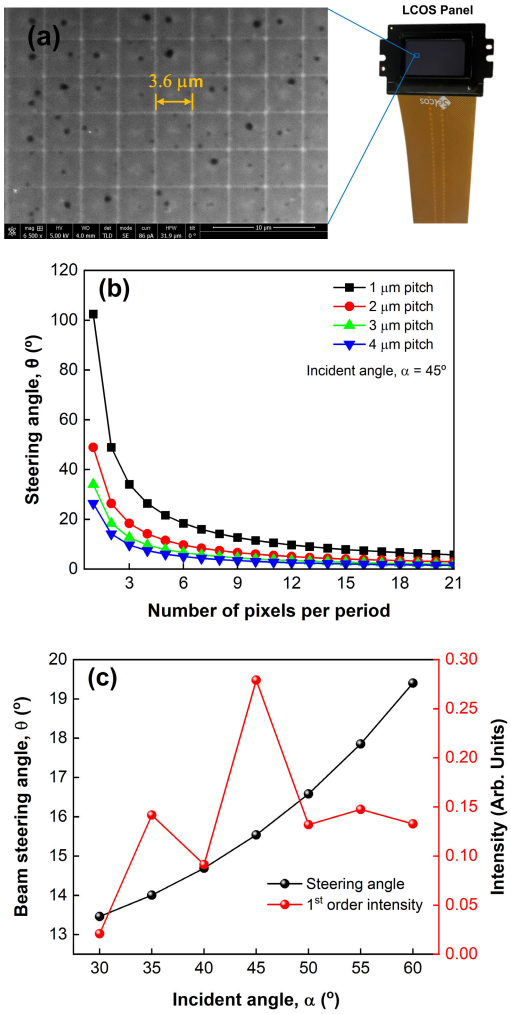

Fig. 2. (a) SEM micrograph of the fabricated LCOS panel (top view). (b) Calculated beam steering angle for different pixel pitches using the grating equation. (c) Simulation results of 1st order beam steering angle with power for incident angle.

segmented metal mirror in each pixel. The pitch of each metal mirror is 3.6 μm as shown in Fig. 2(a). Due to the small gap between the electrodes, the filling factor of LCOS is high. In addition, the diffraction loss due to the mirror discontinuity is low. Fig. 2(b) represents the calculated steering angle of the 1^{st}-order diffraction pattern using the grating equation (1) for different pitches of the LCOS pixel at $\alpha = 45°$. It is evident that the steering angle decreases with increases in the number of pixels or periods. Therefore, the pixel pitch of the LCOS must be small enough to obtain a diffraction pattern with a larger angle, i.e., a wider beam steering angle. Also, we have performed FDTD simulations to find the optimal angle of incidence (α). Fig. 2(c) shows steering angle and the intensity of 1^{st}-order diffraction beam at different incident angles. The efficiency of the 1^{st}-order diffraction is oscillatory and observed highest at $\alpha = 45°$.

III. Experimental Results and Analysis

The schematic representation of the experimental setup is depicted in Fig. 3. To characterize the beam steering angle, a polarization-controlled light emitted from a C-band tunable laser (Agilent 8160) was incident on the LCOS device at a 45°

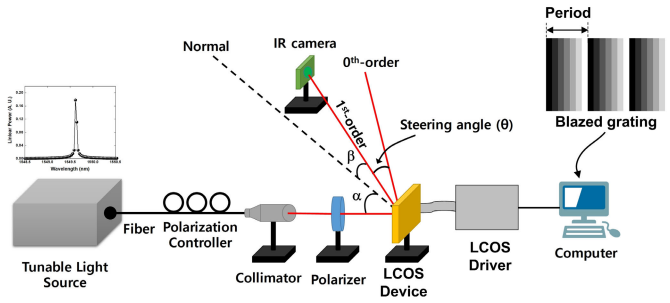

Fig. 3. Schematic diagram of the LCOS device beam steering measurement system.

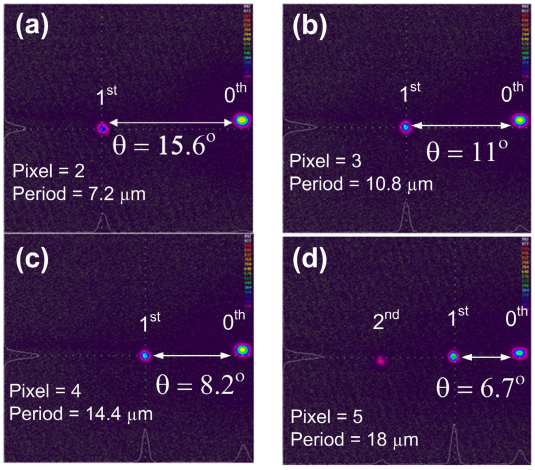

Fig. 4. Experimentally measured far-field diffraction patterns of the steered beam of the proposed LCOS device for different pixel (period) of (a) 2 (7.2 μm), (b) 3 (10.8 μm), (c) 4 (14.4 μm), and (d) 5 (18 μm).

angle of incidence with an input power of 7.45 mW. The input beam diameter of $1/e^2$ is 1.8 mm and cover 196,000 pixels. At this configuration (2 pixels), the measured reflectivity of the LCOS was about 61.9%. A blazed grating-type voltage was applied to the LCOS panel to create a refractive index grating. The applied voltage was controlled by a commercially available display driver. The display driver controls the LCOS through a grayscale image generated by the computer that maps the input voltage signal to each pixel on the LCOS device as shown in Fig. 3. Moreover, our experiments were performed at room temperature.

The 1^{st}-order diffraction beam was steered by changing the period of the grating in the LCOS panel at fixed $\alpha = 45°$. The diffraction pattern was recorded by an infrared camera (Spiricon SP-1550IR) and further evaluated the characteristics of the steered beam using a Fourier image system. The angle between the 0^{th}- and the 1^{st}-orders is considered the steering angle (θ) of the LCOS device. Fig. 4 shows the far-field image of the 1^{st}-order diffraction beam reflected from the LCOS panel by Fourier image system. When the period of the blazed grating, $d = 7.2$ μm (one grating period is equal to two pixels), the measured maximum steering angle was $+15.6°$ with a diffraction efficiency of 2.28%. Further, we have observed the beam steering angles of $+11°$, $+8.2°$ and $+6.74°$ with diffraction efficiencies of 5.64%, 6.11%, 12.79% for d values of 10.8 μm (3 pixels), 14.4 μm (4 pixels), and 18 μm (5 pixels), respectively. This result shows that as we further increased the number of pixels, i.e., the period constituting the

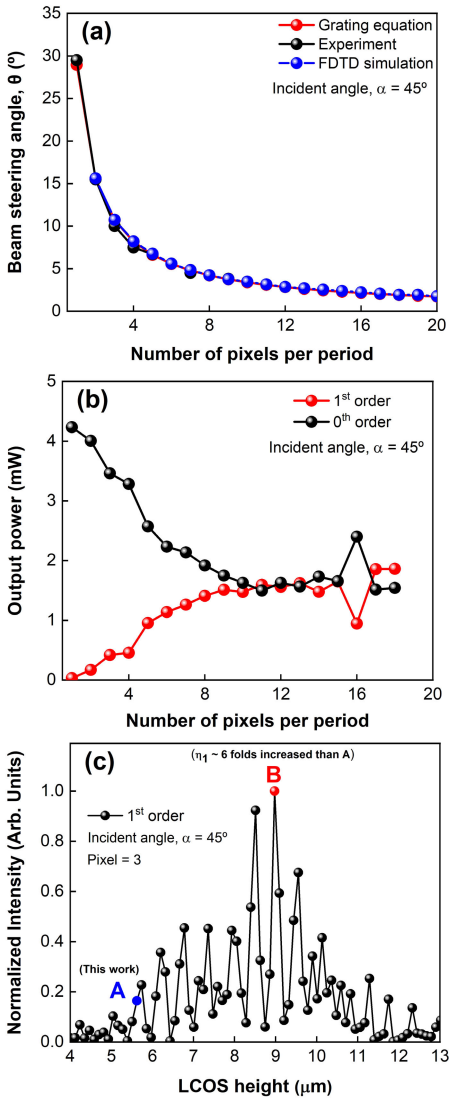

Fig. 5. (a) Comparison of steering angle from the grating equation, experiment, and FDTD simulation at different periods (pixels) of the proposed LCOS device (b) Variation of beam steering power of zeroth- and first-order diffraction patterns at a 45° input beam incident angle. (c) 0^{th} and 1^{st} order power for LCOS height.

blazed grating, the diffraction beam was directed towards the 0^{th}-order. In other words, the beam steering angle decreases with an increase in the LCOS period. Also, the 1^{st}-order diffraction efficiency increased at the cost of a reduced beam steering angle at a higher pixel number. This reduction in diffraction efficiency could be due to the fringing field and crosstalk [21], [22].

To validate the experimental values, we have compared the measured data with the FDTD simulation and grating equation at a fixed $\alpha = 45°$. The measured beam steering angles at different pixels show good agreement with both the calculated values from the FDTD simulation and the grating equation, which is shown in Fig. 5(a). In addition, we have also compared the output power of the 0^{th}- and 1^{st}-orders to understand the power distribution between them at different pixel with constant input power. From Fig. 5(b), it is observed that the output power of the 1^{st}-order at lower pixels is comparatively low compared to that of the 0^{th}-order power. However, as the pixel number increases, the power difference

between the 0^{th}- and 1^{st}-orders becomes minimal at around 10 pixels. At some higher pixels, the 1^{st}-order power was found to be even greater than the 0^{th}-order power. There is a decrease in diffraction power at 16 pixels per period. The cause of this decrease in efficiency is the interference effect due to the angle of incidence and pixel gap.

Conclusively, there is a tradeoff between the diffraction efficiency and pixel number, and consequently, the beam steering angle. Particularly in wide-angle diffraction, the decline in diffraction efficiency is severe because fewer pixels constitute one period. Besides, the insufficient depth of the phase grating also reduces the diffraction efficiency. The depth of the phase grating in this work is 1.4π, which is found not sufficiently enough to provide high diffraction efficiency. To provide more insight on this, we have calculated the beam steering using FDTD simulation by varying the height of the LCOS to provide information on sufficient phase grating depth. Fig. 5(c) shows the simulation results of the far-field intensity of the 1^{st}-order diffraction of LCOS at $\alpha = 45°$ for 3 pixels as a reference. It is confirmed that the low 1^{st}-order diffraction efficiency of the LCOS device in this work is due to the insufficient phase depth at the LCOS height of 5.6 μm, which is represented by point A. It is noticeable that the 1^{st}-order diffraction efficiency was found to be about 6 times higher than our current design at the LCOS height of 8.9 μm represented by point B. This high efficiency is due to the sufficient phase grating depth (over 2π). Therefore, LCs with sufficiently large heights provide high diffraction efficiency. This current research is more focus on increasing the beam steering angle. Our future direction will be based on the improvement of the LCOS design with high efficiency as well as a wider beam steering angle for LiDAR applications.

IV. Conclusion

In this letter, wide beam steering using the LCOS device with a fine pitch of 3.6 μm has been demonstrated for potential future LiDAR applications. Different beam steering angles were achieved at different periods of the LCOS device. A maximum beam steering angle of $\pm 15.6°$ with a 1^{st}-order diffraction efficiency of 2.28% was achieved using this approach at two pixels. Various parameters influencing the beam steering angle of the LCOS device were discussed. Also, the experimental results were verified with the FDTD simulation as well as the grating equation and show good agreement. Through this study, an increase in beam steering angle using LCOS was achieved. Furthermore, it is vital to look for possible ways to increase the efficiency and beam steering angle of the LCOS device with better designs or adaptions such as MEMS or metasurface assisted LCOS-OPA devices for a wider FOV in the near future.

Acknowledgment

The authors would like to thank MAY Company Ltd. (www.selcos.co.kr) for the fabrication of the LCOS device.

References

[1] C.-Y. Chan, "Advancements, prospects, and impacts of automated driving systems," *Int. J. Transp. Sci. Technol.*, vol. 6, no. 3, pp. 208–216, Sep. 2017, doi: 10.1016/j.ijtst.2017.07.008.

[2] M. Galvani, "History and future of driver assistance," *IEEE Instrum. Meas. Mag.*, vol. 22, no. 1, pp. 11–16, Feb. 2019, doi: 10.1109/MIM.2019.8633345.

[3] V. A. Banks, K. L. Plant, and N. A. Stanton, "Driver error or designer error: Using the perceptual cycle model to explore the circumstances surrounding the fatal Tesla crash on 7th May 2016," *Saf. Sci.*, vol. 108, pp. 278–285, Oct. 2018, doi: 10.1016/j.ssci.2017.12.023.

[4] P. S. Argall et al., "LiDAR," in *Encyclopedia of Imaging Science and Technology*. Hoboken, NJ, USA: Wiley, 2022, pp. 869–889.

[5] C. V. Poulton et al., "Coherent solid-state LiDAR with silicon photonic optical phased arrays," *Opt. Lett.*, vol. 42, no. 20, pp. 4091–4094, Oct. 2017, doi: 10.1364/OL.42.004091.

[6] S. Zhao, J. Chen, and Y. Shi, "All-solid-state beam steering via integrated optical phased array technology," *Micromachines*, vol. 13, no. 6, p. 894, Jun. 2022, doi: 10.3390/mi13060894.

[7] D. Wang, C. Watkins, and H. Xie, "MEMS mirrors for LiDAR: A review," *Micromachines*, vol. 11, no. 5, p. 456, Apr. 2020, doi: 10.3390/mi11050456.

[8] A. C. Overvig et al., "Dielectric metasurfaces for complete and independent control of the optical amplitude and phase," *Light, Sci. Appl.*, vol. 8, no. 1, pp. 1–12, Oct. 2019, doi: 10.1038/s41377-019-0201-7.

[9] J. P. B. Mueller, N. A. Rubin, R. C. Devlin, B. Groever, and F. Capasso, "Metasurface polarization optics: Independent phase control of arbitrary orthogonal states of polarization," *Phys. Rev. Lett.*, vol. 118, no. 11, Mar. 2017, Art. no. 113901, doi: 10.1103/PhysRevLett.118.113901.

[10] S.-H. Kim et al., "Thermo-optic control of the longitudinal radiation angle in a silicon-based optical phased array," *Opt. Lett.*, vol. 44, no. 2, pp. 411–414, Jan. 2019, doi: 10.1364/OL.44.000411.

[11] G. Kang et al., "Silicon-based optical phased array using electro-optic *p-i-n* phase shifters," *IEEE Photon. Technol. Lett.*, vol. 31, no. 21, pp. 1685–1688, Nov. 1, 2019, doi: 10.1109/LPT.2019.2939550.

[12] C. Sun et al., "High-efficiency beam steering LCOS for wavelength selective switch," *IEEE Photon. Technol. Lett.*, vol. 30, no. 19, pp. 1683–1686, Oct. 1, 2018, doi: 10.1109/LPT.2018.2866283.

[13] H. Yang and D. P. Chu, "Digital phase-only liquid crystal on silicon device with enhanced optical efficiency," *OSA Continuum*, vol. 2, no. 8, pp. 2445–2459, Aug. 2019, doi: 10.1364/OSAC.2.002445.

[14] D. Yang et al., "Research of two-dimensional beam steering in LCOS-based wavelength selective switch," *Appl. Opt.*, vol. 54, no. 14, pp. 4411–4416, May 2015, doi: 10.1364/AO.54.004411.

[15] S. Qin et al., "Liquid crystal-optical phased arrays (LC-OPA)-based optical beam steering with microradian resolution enabled by double gratings," *Appl. Opt.*, vol. 58, no. 15, pp. 4091–4098, May 2019, doi: 10.1364/AO.58.004091.

[16] Y. Gao, Z. Tan, X. Chen, and G. Chen, "A hybrid algorithm for multi-beam steering of LCOS-based wavelength selective switch," *IEEE Photon. J.*, vol. 12, no. 3, pp. 1–11, Jun. 2020, doi: 10.1109/JPHOT.2020.2990762.

[17] Z. Huang et al., "High-performance beam steering based on liquid crystal on silicon device operating at low bit depths with the maximum efficiency," *Opt. Lasers Eng.*, vol. 156, pp. 1–8, Sep. 2022, doi: 10.1016/j.optlaseng.2022.107083.

[18] Z. Zhang et al., "Fundamentals of phase-only liquid crystal on silicon (LCOS) devices," *Light, Sci Appl.*, vol. 3, pp. 1–10, Oct. 2014, doi: 10.1038/lsa.2014.94.

[19] X. Wang et al., "Liquid-crystal blazed-grating beam deflector," *Appl. Opt.*, vol. 39, no. 35, pp. 6545–6555, Dec. 2000, doi: 10.1364/AO.39.006545.

[20] F. J. Duarte, "Spectrometry and interferometry," in *Tunable Laser Optics*, 1st ed. New York, NY, USA: Academic, 2003, ch. 11, sec. 11.2.2, pp. 227–248.

[21] S. Moser et al., "Model-based compensation of pixel crosstalk in liquid crystal spatial light modulators," *Opt. Exp.*, vol. 27, no. 18, pp. 2506–25046, Aug. 2019, doi: 10.1364/OE.27.025046.

[22] L. Xu, J. Zhang, and L. Y. Wu, "Influence of phase delay profile on diffraction efficiency of liquid crystal optical phased array," *Opt. Laser Technol.*, vol. 41, no. 4, pp. 509–516, Jun. 2009, doi: 10.1016/j.optlastec.2008.07.003.